Raman-susceptibility, damping-constant, and oscillator-strength determination from stimulated polaritons in quartz

S. Biraud-Laval, R. Reinisch, N. Paraire, and R. Laval
Institut d'Electronique Fondamentale, Laboratoire associé au Centre National de la Recherche Scientifique, Université Paris-XI, Bâtiment 220, Centre d'Orsay 91405, France
(Received 13 March 1975)

We study coherent excitation of polaritons by a two-beam method, measuring the amplification of the lower-frequency beam. The experimental polariton dispersion curve is used to get the oscillator strengths for the E modes of quartz. Damping constants and Raman nonlinear coefficients are also determined from a comparison between experimental and theoretical results, including incident-beam spectral width and divergence influence.

I. INTRODUCTION

Quartz has been widely studied in the past, but most of the published results are only qualitative ones. From polariton experiments, we quantitatively determine several parameters for the E modes of quartz: oscillator strengths, damping constants, and nonlinear susceptibilities. These results are obtained by stimulated Raman scattering. The usual way to get stimulated Raman effect is to focus a powerful incident beam inside a medium. A coherent Stokes emission at the frequency corresponding to the maximum gain can be observed, but very often, owing to the high intensity of the incident beam, some crystal damage occurs. In order to avoid this, we use a two-beam method (TBM): two coherent light beams are simultaneously sent into the crystal, and polaritons are excited at the beat frequency. Interaction is then immediately coherent, for any incident power. By this method, we get a selective excitation at any frequency and any wave vector, by varying one of the incident frequencies, and the angle between the two incident beams independently.

On the other hand, TBM is a very convenient method to achieve forward scattering; this is important, since polariton studies require small scattering angles.

We describe here our experimental setup. Measurements are generally performed on the lower-frequency beam (Stokes beam): as the interaction occurs, this beam is amplified. We get an experimental determination of polariton dispersion curves which allows us to calculate the oscillator strength values. Comparison between experimental results and theoretical calculation of the Stokes beam amplification, including the influence of the spectral width and the divergence of the incident beams lead to the determination of damping constants and Raman susceptibilities for each vibration mode.

II. EXPERIMENTAL

Although polaritons excited by TBM are coherent for any power of the incident beams,[1] the nonlinear effects under study become more and more intense as the incident powers increase. So we need two powerful coherent sources, one (at least) being frequency tunable.

The experimental setup is given in Fig. 1. Two dye lasers are simultaneously pumped by a Q-switched ruby laser (20 MW, 30 nsec). The dye is diethyl-thiadicarbocyanine iodide (DTDC), the solvent being ethanol. Each dye laser delivers a 15-nsec pulse, with a peak power of 2–3 MW. The divergence is about 1 mrad, and the spectral width is estimated to 2 cm^{-1}. The polarization is the same as that of the pumping ruby light,[2] and can be adjusted by means of the half-wave plates L. For a difference between the two incident beam frequencies larger than 400 cm^{-1}, we only use one dye laser, the second beam being a part of the ruby laser light.

When the interaction occurs inside the crystal between the two light beams and the polaritons, the higher frequency beam (E_1, ω_1, $\vec{k}_1$) is depleted while the lower frequency one (E_2, ω_2, $\vec{k}_2$) is amplified, as the interaction follows the scheme

photon 1 → photon 2 + polariton.

We measure the power relative variation (PRV) of either the higher-frequency or the lower-frequency beam, as polariton frequency is tuned (Fig. 2). This is done for a constant value of the angle between the two incident beams. The signals given by the two photodiodes $P1$ and $P2$ are compared with a differential amplifier, $P1$ signal

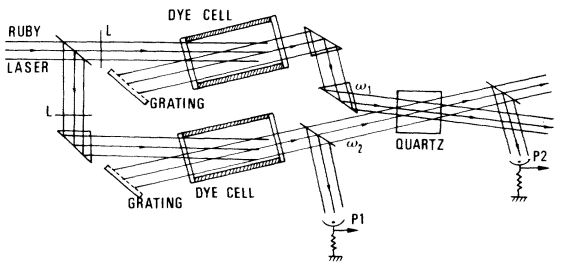

FIG. 1. Experimental setup.

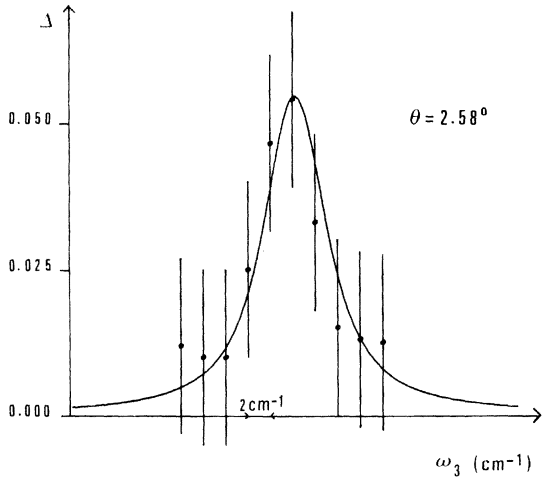

FIG. 2. Power relative variations of the lower-frequency beam vs polariton frequency. The experimental points give a frequency $\Omega_{3\,expt} = 433$ cm^{-1} for the peak position. The integrated-power-variation (Δ) calculated curve (solid line) peak frequency is $\Omega_{3\,th} = 428$ cm^{-1}.

is also used as a power reference. The PRV is maximum for a value Ω_3 of the polariton frequency ω_3, which is known from the dye laser frequencies ($\omega_3 = \omega_1 - \omega_2$). The corresponding polariton wave vector $\vec{k}_3$ can be easily deduced from the value of the angle θ between the two incident beams, and thus we experimentally determine the polariton dispersion curves.[3]

This is done here for a quartz crystal. In order to observe only E modes and to use quartz birefringence to achieve the phase-matching condition, we choose a α_{xz} scattering geometry. The higher-frequency beam ($\vec{E}_1$) is polarized along the x axis and always propagates along the normal y to the crystal front face; the lower frequency one ($\vec{E}_2$) is polarized along the optical axis z and propagates in the xy plane. Under these conditions, the polariton wave vector also lies in the xy plane, and we can observe the ordinary polariton modes (purely transverse), and the longitudinal phonon modes. The experimental points for the dispersion curve are shown in Fig. 3. The PRV maximum intensity and its spectral width (Fig. 2) are also measured, and will be compared with the theoretical values.

III. CALCULATION AND DISCUSSION

With the geometrical conditions described in Sec. II, we can calculate the theoretical expression of the relative amplification of the lower-frequency beam $\Delta W_{2z}/W_{2z}$ from the propagation equations for the electric fields at frequencies ω_1, ω_2, and ω_3, and the ion-motion equation. The detailed calculation is reported in Ref. 4. In this calculation, we take care of the fact that the polariton field $\vec{E}_3$ has a nonzero divergence. Then, the expression of the power variation thus obtained include scattering from the longitudinal phonon modes. We get the following approximate expression:

$$\frac{\Delta W_{2z}}{W_{2z}} = \frac{2\omega_2}{\epsilon_0 c^2 n_{1x} n_{2z}} \times \mathrm{Im}\left((2\chi_{yxz})^2 \frac{\omega_3^2}{c^2} \frac{k^2 - k_{3y}^2}{k^2(k^2 - k_3^2)} - \chi_R\right) L\, W_{1x}\,, \quad (1)$$

where n_{1x} and n_{2z} are the refractive indices of quartz for the fields E_1 and E_2, respectively. χ_{yxz} and χ_R are elements of nonlinear susceptibility and Raman susceptibility tensors, L being the crystal thickness, and W_{1x} the incident power of the ω_1 beam. $\vec{k}$ and $\vec{k}_3$ are wave vectors of the free and driven waves which propagate in the crystal at frequency ω_3. k is given by the usual complex dispersion relation

$$\frac{k^2 c^2}{\omega_3^2} = \epsilon_\infty + \sum_m \frac{S_m \omega_m^2}{\omega_m^2 - \omega_3^2 + j\omega_3 \omega_m \gamma_m}\,,$$

and $\vec{k}_3$ is defined by $\vec{k}_3 = \vec{k}_1 - \vec{k}_2$.

In this calculation, we assumed each of the two incident beams strictly monochromatic (with frequencies ω_1 and ω_2, respectively) and we neglected any divergence, considering a well-defined wave

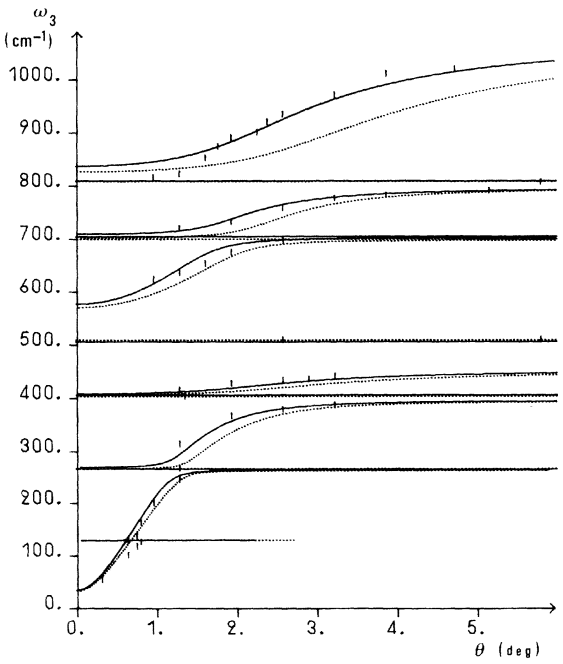

FIG. 3. Polariton dispersion curve for E modes of quartz. Dotted lines: theoretical curves obtained with oscillator strength values from Refs. 6 and 7. Solid lines: theoretical curves obtained by fitting the experimental points. Vertical lines: experimental results.

TABLE I. Oscillator strengths, longitudinal frequencies, damping constants, and nonlinear Raman coefficients for the E modes of quartz.

ω_m (cm^{-1})	S_m	γ_m	$(A_m)_{yxz}$ (10^{-10} mksA)	Longitudinal frequencies (cm^{-1}) measured	calculated
128.4	0.007	0.054	2.4	...	...
265	0.071	0.017	2.9	266	267
395	0.29	0.008	1.7	402	405
452	0.60	0.016	3.8	509	504
702	0.018	0.009	6.2	...	704
797	0.084	0.013	3.8	807	809
1072	0.33	0.007	−3.0	...	1143
1163	0.01	...	−5.1	...	1175

vector for each beam (with incidence angles θ_1 and θ_2).

To get an accurate comparison with experiments, we must take into account the spectral width and spatial divergence of the two incident beams. This is done, assuming Gaussian distributions over the the $\omega_{1,2}$ and $\theta_{1,2}$ ranges, with central values $\omega^0_{1,2}$ and $\theta^0_{1,2}$, and halfwidths $\Delta\omega_{1,2}$ and $\Delta\theta_{1,2}$. $\Delta W_{2z}/W_{2z}$ slowly varies with ω_2, but mainly depends on $\omega_3=\omega_1-\omega_2$ and on the driven wave vector k_3. We have already mentioned that k_3 is closely related to the angle $\theta=\theta_1-\theta_2$ between the incident rays. We thus obtain the following expression for the integrated power variation (Δ):

$$\Delta=[\pi(\Delta\omega_1^2+\Delta\omega_2^2)^{1/2}(\Delta\theta_1^2+\Delta\theta_2^2)^{1/2}]^{-1}\times\iint\frac{\Delta W_{2z}(\omega_3,\theta)}{W_{2z}}\exp\left(-\frac{(\omega_3-\omega_3^0)^2}{\Delta\omega_1^2+\Delta\omega_2^2}\right)\times\exp\left(-\frac{(\theta-\theta^0)^2}{\Delta\theta_1^2+\Delta\theta_2^2}\right)d\omega_3\,d\theta. \tag{2}$$

This expression is numerically computed and allows a comparison between theoretical and experimental values.

The Raman susceptibility χ_R appearing in (1) can be written[4]

$$\chi_R=\sum_m\frac{A_m^2\omega_m^2\gamma_m}{\omega_m^2-\omega_3^2+j\omega_3\omega_m\gamma_m}, \tag{3}$$

where A_m^2 characterizes the contribution to χ_R of the resonant term at frequency ω_m; γ_m is the reduced damping constant. We also get[4] for the nonlinear susceptibility χ_{yxz},

$$\chi_{yxz}=\frac{1}{2}\sum_m\frac{A_m\omega_m(\gamma_m S_m)^{1/2}}{\omega_m^2-\omega_3^2+j\omega_3\omega_m\gamma_m}. \tag{4}$$

S_m is the oscillator strength for the mth optical mode.

The frequencies ω_m are experimentally determined.[3] Δ contains three other sets of eight parameters (quartz has eight E modes[5]): the oscillator strengths S_m, the damping constants γ_m, and the parameters A_m (closely related to the Raman susceptibilities).

A. Oscillator strength determination

We show in Ref. 4 that the dispersion curves can be accurately described by the relation

$$\frac{k_3^2c^2}{\omega_3^2}=\epsilon_\infty+\sum_m\frac{S_m\omega_m^2}{\omega_m^2-\omega_3^2}. \tag{5}$$

The oscillator strengths S_m have been previously determined from ir techniques.[6,7] With these ir S_m values, we draw the dispersion curves which are the dotted lines in Fig. 3. These curves do not agree with Raman scattering results. This discrepancy was already present in Ref. 8, in particular for polaritons associated with the 1072-cm^{-1} mode.

We use dispersion relation (5) to fit the theoretical dispersion curve with our experimental one taking into account both transverse and longitudinal modes (with $k_3=0$ for the latter ones). The best fit is obtained with the values given in Table I, and the corresponding curves are drawn in solid lines in Fig. 3. The agreement between our theoretical dispersion curve and the experimental points is quite satisfactory for most of the observed modes, especially in the 800–1072-cm^{-1} range where the initial discrepancy was the largest. The longitudinal frequencies calculated with these S_m values are reported in Table I. We note that a good agreement cannot be simultaneously obtained on the transverse polariton branch associated to the phonon at 1072 cm^{-1} and on the two highest longitudinal frequencies for any set of S_m values.

Although the oscillator strengths we obtain are rather different from those determined from ir measurements by Spitzer and Kleinman[6] for frequencies larger than 270 cm^{-1} and Russell and Bell[7] for frequencies lower than 500 cm^{-1}, the ir reflectivity calculated at normal incidence with our S_m values is found to be equal to Spitzer and Kleinman's results within 10%.

B. Damping constants and nonlinear susceptibilities

Let us now consider relation (1) for ω_3 in the vicinity of ω_m. The driven wave vector k_3 is then very different from the free one k, thus all terms excepted the last one vanish. Neglecting every nonresonant term in χ_R, we get

$$\left(\frac{\Delta W_{2z}}{W_{2z}}\right)_m=\frac{2\omega_2}{\epsilon_0c^2n_{1x}n_{2z}}\frac{A_m^2\omega_m^3\omega_3\gamma_m^2}{(\omega_m^2-\omega_3^2)^2+\omega_3^2\omega_m^2\gamma_m^2}LW_{1x}. \tag{6}$$

From experiments, we know the intensity and spectral width of the power relative variation and this is used together with (6) and (2) to determine the values of γ_m and A_m in the following way.

From Eq. (6), it is obvious that the halfwidth is independent of A_m. The γ_m are numerically ad-

justed to give to the Δ variations in the vicinity of ω_m a spectral width equal to the experimental one. This is done for each mode independently, and the results are reported in Table I.

Approximate values are calculated for $|A_m|$ using Eq. (6) and the measured PRV maximum intensity obtained at $\omega_3 = \omega_m$. These values are then improved using the whole polariton range results. For calculation convenience, we consider that the measured PRV maximum intensity corresponds to the theoretical frequency $\Omega_{3\,\mathrm{th}}$, determined from the calculated dispersion curve, instead of the experimental value $\Omega_{3\,\mathrm{expt}}$.

The parameters A_m can be either positive or negative. But we can note from Eqs. (1), (3), and (4) that it is only possible to determine their relative signs. Quartz has eight E modes, so 2^7 sign combination will be considered. For each sign combination, using the $|A_m|$ approximate values, the Δ peak values are computed over the whole polariton frequency range, and compared to the corresponding measured values of PRV.

Computation results show that most of the sign combinations give a discrepancy between theoretical and experimental values of the power variation peaks in the 820–1072-cm^{-1} range. In this range, a good fit is only obtained with the following sign combination for A_4, A_5, A_6, $A_7 = +++-$, whatever the signs are for the parameters A_1, A_2, A_3 associated to the three lower-frequency modes. The sign of A_8, corresponding to the phonon at 1163 cm^{-1} is not crucial, nevertheless, results are slightly improved near 1072 cm^{-1} when A_8 is negative. The signs of A_1, A_2 and A_3 are determined by comparing the Δ and PRV peak values in the corresponding range (0– 400 cm^{-1}). The best fit is obtained when these three parameters are positive. Thus, we retain the following sign combination: $+++++--$. The $|A_m|$ values are then more accurately adjusted to get the best agreement with experimental data. Results are given in Table I. The corresponding curve and experimental points are drawn on Fig. 4.

The uncertainty about $|A_m|$ values is mainly due to the incident beam power fluctuations and the beam intersection adjustment (which is delicate, as we are working with 20-nsec nonrecurrent pulses). It is roughly estimated to 20%.

The curve given in Fig. 4 can be compared to the graph given by Scott and Ushioda[9] who studied spontaneous Raman effect in quartz and reported the variations of theoretical polariton scattering intensities: they exhibit nearly the same behavior for polaritons associated with the phonons at 1072 and 797 cm^{-1}: Δ increases as frequency is lowered from 1072 to 900 cm^{-1}; it then goes through zero at 754 cm^{-1}. However, they are different concerning the polaritons associated with the phonons at 128 and 265 cm^{-1}: the ratio between the peak values for these two modes is different, and Δ remains rather small. Two factors can explain this discrepancy. At first, the Bose population factor $[n(\omega)+1]$, which only appears in spontaneous Raman scattering efficiency, contributes to enhance the intensities of the lowest-frequency modes in Scott and Ushioda's results. But the main factor is the beam divergence, the influence of which increases when the maxima of $\Delta W_2/W_2$ become sharper. Besides, maxima of $\Delta W_2/W_2$ are all the more sharp as the slope of the dispersion curve is larger, and consequently the influence of divergence, which was negligible for the higher-frequency modes, is particularly important for the two lowest-frequency modes of quartz. If we consider the stimulated Raman scattering efficiency, or $\Delta W_2/W_2$, we find that the largest values occur for polaritons associated with phonon at 128 cm^{-1}, but as this mode shows also the sharpest maxima for $\Delta W_2/W_2$, the corresponding Δ is then smaller than for the second mode.

In the 300–700 cm^{-1} range, the relative intensities for xy and xz scattering have opposite variations.[9] A slight misorientation of the crystal would give rise to a mixture of polarizability com-

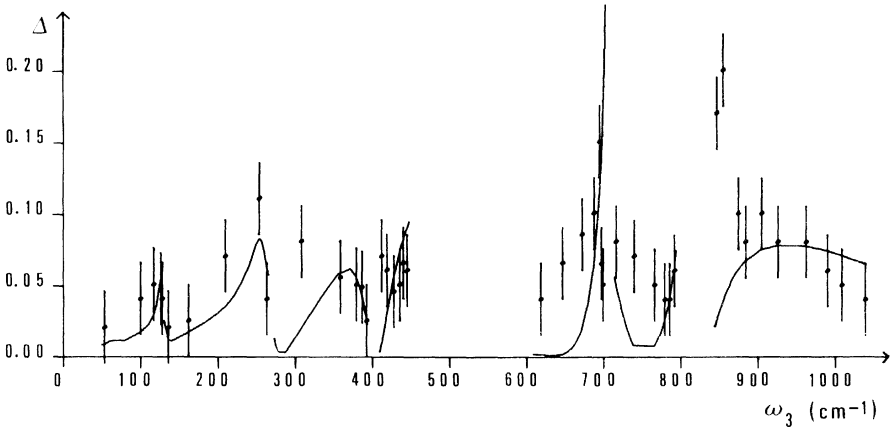

FIG. 4. Measured and calculated peak values of the power relative variations vs polariton frequency. Vertical lines: experimental results.

ponents and this could explain some disagreement between our results and the earlier ones of Ref. 9 near 400 and 700 cm^{-1}.

The beam divergence, as well as the spectral linewidth, also acts on the observed linewidth. Knowing the A_m and γ_m values, we have calculated the Δ line shape in the polariton range. The spectral linewidths for different points of the dispersion curve are in good agreement with the experimental ones. An example is given in Fig. 2. We also observe that the theoretical linewidth (as well as the experimental one) decreases at large angles, i.e., where the dispersion curve is nearly flat. Two factors contribute to this behavior: an intrinsic one, which comes from the relative slopes of the dispersion curve and the θ = constant curves in the (ω, k) diagram; and an external one, related to the beam divergence. When the dispersion curve becomes flat, the beam angular spread influence disappears and the linewidth decreases.

IV. CONCLUSION

We pointed out that in order to correctly describe the experimental results it is important to take into account the incident beam nonmonochromaticity and divergence. Indeed, considering only the simple power variation $\Delta W_2/W_2$, given by relation (1), would lead to very different and erroneous values for the nonlinear susceptibilities A_m, essentially for their relative signs.

Coherent excitation of polaritons by TBM appears as a way to determine the oscillator strengths, damping constants and nonlinear susceptibilities of a crystal.

ACKNOWLEDGMENTS

We would like to thank Dr. G. Chartier who initiated this work, and Dr. P. M. Janot for many helpful discussions and suggestions regarding the computer calculations.

[1]R. Reinisch, S. Biraud-Laval, G. Chartier, and N. Paraire, Phys. Rev. B 9, 1861 (1974).
[2]R. Laval, thèse d'ingénieur (CNAM, Paris, 1974) (unpublished).
[3]S. Biraud-Laval, J. Phys. (Paris) 35, 513 (1974).
[4]R. Reinisch, S. Biraud-Laval, N. Paraire, J. Phys. (Paris) 37, 051 (1976).
[5]H. Poulet and J. P. Mathieu, *Spectres de Vibration et Symêtrie des Cristaux* (Gordon and Breach, New York, 1970).
[6]W. G. Spitzer and D. A. Kleinman, Phys. Rev. 161, 1324 (1961).
[7]E. E. Russell and E. E. Bell, J. Opt. Soc. Am. 57, 341 (1967).
[8]J. F. Scott, L. E. Chessman, and S. P. S. Porto, Phys. Rev. 162, 834 (1967).
[9]J. F. Scott and S. Ushioda, *Light Scattering Spectra of Solids* (Springer-Verlag, New York, 1969).